Redox Biology 15 (2018) 228–242

Contents lists available at ScienceDirect

Redox Biology

journal homepage: www.elsevier.com/locate/redox

Research paper

Apolipoprotein A-1 mimetic peptide 4F promotes endothelial repairing and compromises reendothelialization impaired by oxidized HDL through SR-B1

Dan He[a,1], Mingming Zhao[a,1], Congying Wu[b], Wenjing Zhang[c], Chenguang Niu[a], Baoqi Yu[a], Jingru Jin[c], Liang Ji[a], Belinda Willard[d], Anna V. Mathew[e], Y. Eugene Chen[e], Subramaniam Pennathur[e], Huiyong Yin[f], Yuan He[g], Bing Pan[a,*], Lemin Zheng[a,*]

[a] The Institute of Cardiovascular Sciences and Institute of Systems Biomedicine, School of Basic Medical Sciences, Key Laboratory of Molecular Cardiovascular Sciences of Ministry of Education, Health Science Center, Peking University, Beijing 100191, China
[b] The Institute of Systems Biomedicine, Department of Medical Genetics, Peking University Health Science Center, Beijing 100191, China
[c] The Military General Hospital of Beijing, Beijing 100700, China
[d] Proteomics Laboratory, Cleveland Clinic, Cleveland, OH 44195, USA
[e] Department of Medicine, University of Michigan, Ann Arbor, MI 48109, USA
[f] Key Laboratory of Food Safety Research, Institute for Nutritional Sciences (INS), Institutes for Biological Sciences (SIBS), Chinese Academy of Sciences (CAS), Shanghai 200031, China
[g] National Research Institute for Health and Family Planning, Beijing 100081, China

ARTICLE INFO

Keywords:
ApoA-1
4F
Endothelial repair
Oxidized HDL
Re-endothelialization

ABSTRACT

Disruption of endothelial monolayer integrity is the primary instigating factor for many cardiovascular diseases. High density lipoprotein (HDL) oxidized by heme enzyme myeloperoxidase (MPO) is dysfunctional in promoting endothelial repair. Apolipoprotein A-1 mimetic 4F with its pleiotropic benefits has been proven effective in many *in vivo* models. In this study we investigated whether 4F promotes endothelial repair and restores the impaired function of oxidized HDL (Cl/NO_2-HDL) in promoting re-endothelialization. We demonstrate that 4F and Cl/NO_2-HDL act on scavenger receptor type I (SR-B1) using human aorta endothelial cells (HAEC) and SR-B1 $^{(-/-)}$ mouse aortic endothelial cells. Wound healing, transwell migration, lamellipodia formation and single cell migration assay experiments show that 4F treatment is associated with a recovery of endothelial cell migration and associated with significantly increased endothelial nitric oxide synthase (eNOS) activity, Akt phosphorylation and SR-B1 expression. 4F increases NO generation and diminishes oxidative stress. *In vivo*, 4F can stimulate cell proliferation and re-endothelialization in the carotid artery after treatment with Cl/NO_2-HDL in a carotid artery electric injury model but fails to do so in SR-B1$^{(-/-)}$ mice. These findings demonstrate that 4F promotes endothelial cell migration and has a potential therapeutic benefit against early endothelial injury in cardiovascular diseases.

1. Introduction

High Density Lipoprotein (HDL) levels demonstrate an inverse relation with incidence of coronary artery disease [1]. In addition to its primary action of reverse cholesterol transport [2] that causes atherosclerosis plaque regression [3–6], HDL has pleiotropic traits like anti-inflammatory [7–11], anti-oxidative [12,13], and anti-apoptotic properties [13,14]. HDL plays an essential role in maintaining endothelial monolayer integrity preventing endothelial dysfunction and injury in response to shear stress from disturbed flow patterns. This disruption of the endothelial monolayer integrity plays a crucial role in the initiation and propagation of atherosclerosis [15] and can be alleviated by the proliferation of neighboring endothelial cells (EC) and endothelial progenitor cells (EPC) [16–18]. HDL promotes endothelial repair by upregulating endothelial nitric oxide (NO) synthase (eNOS) and endothelium-dependent vasodilation [7,19], stimulation of endothelial

List of abbreviations: ApoA-1, Apolipoprotein A-1; Cl/NO_2-HDL, oxidized HDL; Cl-HDL, chlorinated HDL; NO_2-HDL, nitrated HDL; ECM, endothelial cell medium; eNOS, endothelial nitric oxide synthase; EPC, endothelial progenitor cell; HAECs, human aorta endothelial cells; HDL, high density lipoprotein; HETEs, hydroxyeicosatetraenoic acids; HODEs, hydroxyoctadecadienoic acids; HRP, horseradish peroxidase; HUVECs, human umbilical vein endothelial cells; LysoPC, lysophosphatidylcholine MAECs, mouse aortic endothelial cells; MPO, myeloperoxidase; PON1, paraoxonase-1; PCNA, proliferating cell nuclear antigen; ROS, reactive oxygen species; SR-B1$^{+/+}$, SR-B1 wild-type; SR-B1$^{-/-}$, SR-B1 deficient

* Correspondence to: No. 38 Xueyuan Road, Haidian District, Beijing 100191, China .
E-mail addresses: panbintz@163.com (B. Pan), zhengl@bjmu.edu.cn (L. Zheng).
[1] Dan He and Mingming Zhao contributed equally to this work.

https://doi.org/10.1016/j.redox.2017.11.027
Received 25 September 2017; Received in revised form 24 November 2017; Accepted 29 November 2017
Available online 08 December 2017

cell proliferation and migration [20–22] and EPC-mediated endothelial repair [20,23,24]. Also, HDL mediates re-endothelialization by promoting differentiation, inhibition of apoptosis, and dhesion of circulating EPC [25,26].

Scavenger receptor-B type-I (SR-BI) on endothelial cells are directly involved in HDL signaling by promoting endothelial cell migration and re-endothelialization in addition to its traditional function of mediating cholesterol and phospholipid movement between its ligands and cells [18]. This process is nitric oxide independent activation of Rac GTPase through the receptor and dependent on activation of src kinase, phosphatidylinositol 3-kinase, and p44/42 mitogen-activated protein kinase. Human EPC also express surface HDL receptor ecto-F1-ATPase

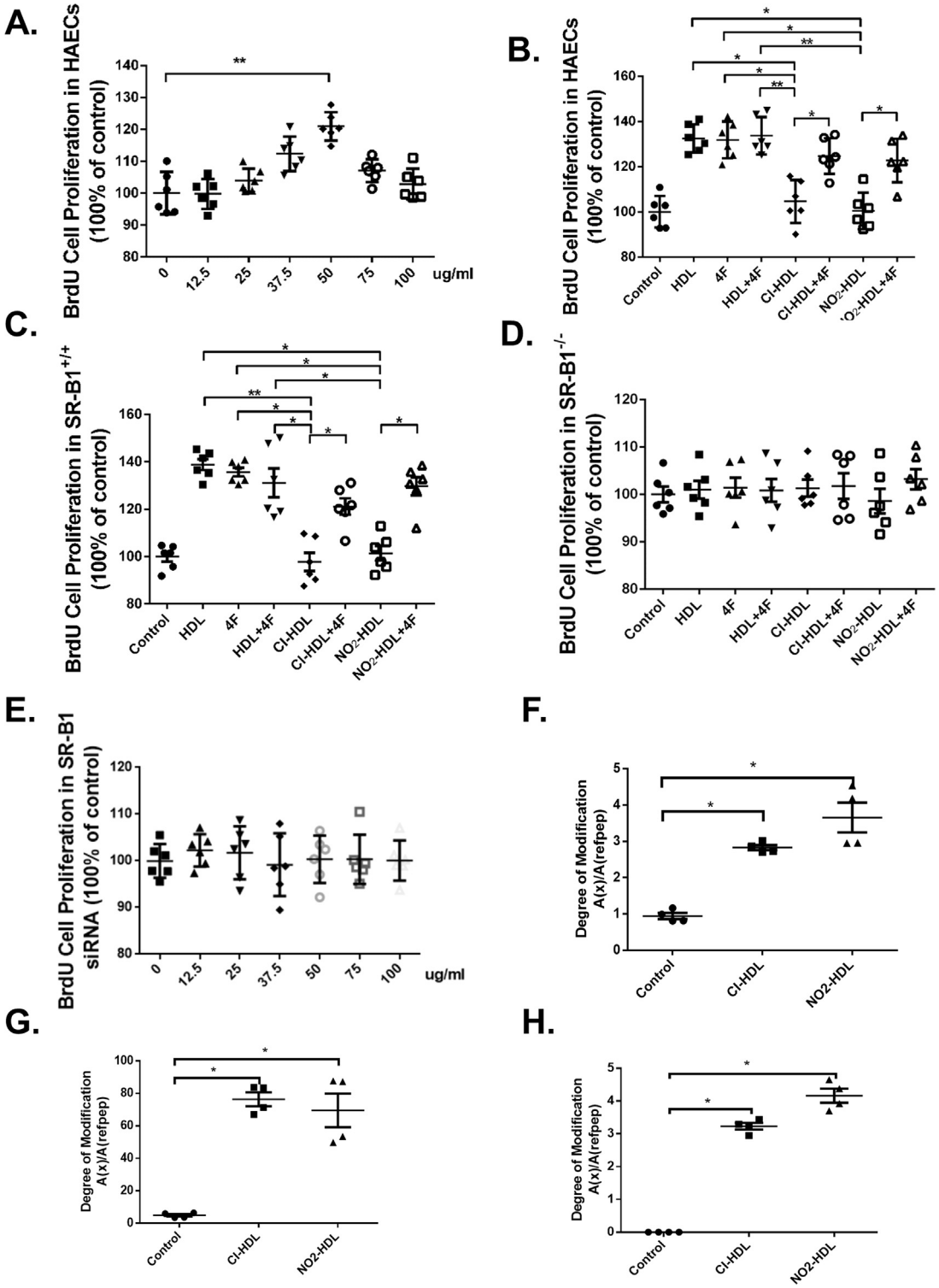

Fig. 1. Effects of 4F and SR-B1 on HAECs proliferation and Cl/NO_2-HDL function. HAECs were treated with 4F for 24 h at varying 4F concentrations in the range of 0–100 μg/mL. Relative cell proliferation was measured by BrdU cell proliferation assay (A). HAECs (B), aortic endothelial cells of SR-BI $^{(+/+)}$ mice (C), aortic endothelial cells of SR-BI $^{(-/-)}$ mice (D) and HAEC treated with SR-B1 siRNA (E). HDL oxidation (F) of tryptophan, (G) methionine, and (H) tyrosine were measured and expressed as oxidized apolipoprotein A-1 to native apolipoprotein A-1 ratios. The experiments had six independent biological replicates and every replicate have three technical replicates each. MAECs experiments were performed from three batches, and cells in each batch were isolated from three mice.

and apolipoprotein A1 (apoA-1), enhance proliferation of human EPC and promotes angiogenesis through the cell surface ATP synthase [26]. Besides, apoA-1 has a significant direct effect on re-endothelialization by increasing differentiation of lineage minus bone marrow-derived cells into CD31 + cells, improving adhesion of the CD31 + cells to vessel wall [24] and contributing to the migration of bone marrow-derived EPC to the damaged endothelium or ischemic tissues.

Paraoxonase 1 (PON1), an atheroprotective protein, has been linked to the anti-oxidative, anti-inflammatory, and lipid cargo–carrying functions of HDL. Like PON1, leukocyte-derived heme protein myeloperoxidase (MPO) relates to HDL, oxidant stress, and atherosclerosis mechanistically. Site–specific MPO mediated chlorination and nitration of apoA-1 residues impair HDL function [27,28]. MPO mediated Cl/NO_2-HDL is dysfunctional and associated with incident and prevalent atherosclerotic disease in many clinical studies [27,29]. Specifically, MPO-catalyzed nitration or chlorination of HDL is a negative modulator of EC proliferation and migration and is unsuccessful in promoting endothelial repair [7,20]. Also, Cl/NO_2-HDL in various disease states can also markedly impair its ability to stimulate endothelial NO production as well as diminish EPC's function in endothelial repair by activation of CD36-MAPK-TSP-1 pathways [29–31]. In light of the significant impairment of the endothelial protection and repair capabilities by dysfunctional HDL, apoA-1 mimetic peptides might possess properties to restore the endothelial protection function of HDL.

ApoA-1 mimetic peptide 18A (18 amino acids;D-W-L-K-A-F-Y-D-K-V-A-E-K-L-K-E-A-F) was first designed and synthesized by Segrest et al. in 1985 [32]. 18A does not have any sequence homology to apoA-1 but mimics the class A amphipathic helixes contained in apoA-1 and thus retains many of the lipid binding properties of apoA-1 [33,34]. Various kinds of apoA-1 mimetic peptides with differing numbers of phenylalanine residues placed at different positions have been synthesized. These series of peptides are named according to the number and location of the phenylalanine residues. Hence 4F (Ac-F [3,14] 18A-NH_2) is a peptide with four phenylalanine residues (at positions 3, 6, 14, and 18) on the hydrophobic end. 4F exhibits optimal hydrophobicity to interact with phospholipids and thus behaves most like apoA-1 in lipid-peptide interactions [35–37]. 4F can promote cholesterol efflux and improve pathological processes in a variety of animal models while exerting pleiotropic effects including anti-inflammatory, anti-oxidant, anti-thrombotic, and lipopolysaccharide protection [35,37–42]. Clinical trials have demonstrated doses of 4F peptide ranging between 40 and 100 mg/kg/day would be required for maximal efficacy in preventing atherosclerosis [34,43,44]. Of note, some studies indicate that 4F can bind oxidized lipids such as hydroxyeicosatetraenoic acids (HETEs) and hydroxyoctadecadienoic acids (HODEs) with even higher affinity than apoA-1 and it may also have the potential to normalize the composition and function of the dysfunctional HDL [40,45–47]. Besides 4F promotes eNOS activation and NO production in human coronary artery endothelial cells, and protects against myocardial infarction through eNOS pathway in C57BL/6J mice.

While it is evident that HDL possesses endothelial protective function and oxidized HDL fails to perform these functions, the role apoA-1 mimetic peptide, 4F in rescuing HDL's protective role in endothelial repair is unknown. The present study explores the role of 4F playing in endothelial repair and extends previous observations by investigating the potential effects of 4F in restoring impaired re-endothelialization by Cl/NO_2-HDL. To this end, both *in vitro* and *in vivo* experiments were designed and executed to delineate the effect of 4F on endothelial repair in the presence of HDL oxidized by MPO. We tested the hypothesis that 4F can restore the impaired function of Cl/NO_2-HDL in re-endothelialization and improve proliferation, migration, and lamellipodia formation of endothelial cells, thus promoting endothelial repair.

2. Methods

2.1. Animals

Five to six-week-old male SR-BI $^{(+/+)}$ mice and SR-BI $^{(-/-)}$ mice on a C57BL/6 background were obtained from Dr. George Liu (Peking University). Genotyping was confirmed using genomic DNA extracted from tails by PCR (Supplemental Fig. 2E). Both mutants and control animals were littermates from heterozygous crosses mating. Five to six-week-old male C57 BL/6 mice were obtained from Department of Laboratory Animal Science, Peking University Health Science Center. All mice were maintained with ad lib access to pellet food and water. Animal husbandry and experimental procedures were carried out strictly by the ethical regulations enforced and approved by the Ethics Committee of Animal Research, Peking University Health Science Center, and conformed to the Guide for the Care and Use of Laboratory Animals (National Institutes of Health).

2.2. Isolation of HDL

Fasting plasma was obtained from peripheral blood of healthy and coronary artery disease subjects. Written informed consent was obtained from every participant before the study began, and the local ethics committee approved the protocol conforming to the declaration of Helsinki. LDL(1.019–1.063 g/mL) and HDL (1.063–1.210 g/mL) were isolated from fresh plasma by ultracentrifugation at 550,000 g for 5 h at 4 °C. The lipoprotein fractions were then dialyzed against phosphate-buffered saline (PBS: 10 mM; Ph 7.4) containing 100 μM diethylenetriamine pentaacetic acid (Sigma, USA) without endotoxin for three days in the dark at 4 °C based on published protocols [20]. The purity of HDL was confirmed by the 12% sodium dodecyl sulfate polyacrylamide gel electrophoresis. HDL was sterilized with 0.22 μm filter, stored in sealed tubes in dark and used within two months. The concentration of HDL was measured by nephelometry (Dimension XPand, Dade Behring, Germany).

2.3. HDL nitration and chlorination catalyzed by MPO in vitro

HDL nitration and chlorination were carried out with MPO as previously described [48]. Briefly HDL was incubated in 60 mM endotoxin-free PBS (Ph 7.0) containing 100 μM diethylenetriamine pentaacetic acid, 500 μg/mL HDL protein, 57 nM MPO, and either 1 mM $NaNO_2$ (for the nitration reaction to produce NO_2-HDL) or 100 mM NaCl (for the chlorination reaction to produce Cl-HDL). The MPO was added at the start of the reactions, hydrogen peroxide (H_2O_2) at 100 mM in 4 aliquots was added at 25 min intervals at 37 °C, and the mix was incubated for a total of 160 min. Then, 2 mM L-methionine was added to quench the reaction for 25 min. Finally, after MPO modification, HDL was dialyzed against 3 × 1 L of endotoxin-free PBS. UV detection at 240 nM revealed that there was no detectable H_2O_2 after this procedure and HDL modification level was measured by mass spectrometry system [20,48] (Fig. 1F–H). The native reference peptide (NRP) method is an LC/MS-based technique that quantifies modified peptides present in a tryptic digest by utilizing an unmodified peptide from the protein of interest that is also formed in the tryptic digestion as the internal standard (native reference peptide). The chromatographic peak areas of the peptides of interest are determined relative to the chromatographic peak area of the native reference peptide as an index of the relative amounts of these analyte peptides. Changes in this ratio represent the changes in the degree of modification. Then, Cl-HDL and NO_2-HDL were sterilized with a 0.22 μm filter and stored at 4 °C in the dark.

2.4. Isolation and cell culture of human umbilical vein endothelial cells (HUVECs)

HUVEC were isolated by collagenase digestion of umbilical veins

from three pooled fresh cords, and all experiments were performed from the same batch. Written informed consent for the use of the umbilical cords for the isolation and culture of the HUVECs was obtained from every participant, and the local ethics committee approved the protocol which was performed conforming to the declaration of Helsinki [49]. Briefly, the vein was rinsed three times with 4-(2-hydroxyethyl)-1-piperazineethanesulfonic acid buffer after perfusion of the vein with a metal gauge. Endothelial cells were digested from the vein walls by collagenase type IA (Sigma; 100 U/mL) at 37 °C for 15 min. The reaction was then terminated by adding Endothelial Cell Medium (ECM; Sciencell, USA). The cell pellet was resuspended in ECM after centrifugation for 5 min at 1000 rpm and the cells were reseeded onto the collagen-coated culture dishes. HUVEC were cultured with ECM containing 5% bovine serum, 1% endothelial cell growth supplement, and 1% penicillin/streptomycin solution, in a humidified atmosphere (5% CO_2) at 37 °C. HUVECs were isolated from three umbilical cords and passages 2–5 were used in all experiments. Anti-CD31 and anti-CD34 antibodies were used to identify endothelial cell phenotype.

2.5. Isolation and cell culture of MAECs

Mouse aortas were excised under anesthesia with inhalation of 2.5% isoflurane to isolate MAECs. The adequacy of anesthesia was monitored through pinching the hind paw, and the sufficiently sedated mice were euthanized by cervical dislocation. Mouse aortas were separated with sterilized devices and 2 mm sections were dissected and placed on matrigel pre-coated plates and cultured in ECM at 37 °C for 7–14 days to promote MAEC outgrowth before passage. The relevant experiments were performed on MAEC cells from three batches at passages 2–3, and cells in each batch were isolated from three mice. The cells were stained with anti-CD31 and anti-CD34 antibodies to confirm endothelial cell phenotype.

2.6. Cell proliferation by 5′-bromo-2′-deoxyuridine (BrdU) immunohistochemistry

HAECs were purchased from ScienCell Research Laboratories (USA), and cultured in ECM as above. HAECs used in all experiments were at passages 3–5 from the same purchase. HAEC were plated at a density of 1000 cells/well in a 96-well plate and were cultured overnight. The cells were incubated with HDL, 4F (D-4F; GL Biochem(Shanghai) Ltd.), HDL + 4F, Cl-HDL, Cl-HDL + 4F, NO_2-HDL, or NO_2-HDL + 4 F for 24 h (native HDL, Cl/NO_2-HDL at 100 μg/mL apoA-1 and 4F at 50 μg/mL concentration). Then cells were labeled with 20 μL/well BrdU labeling solution [20] and incubated with 200 μL/well fixing and denaturing solution. After incubation with 100 μL/well anti-BrdU-POD working solution for 90 min, the cells were washed three times with PBS subsequently, and TMB substrate solution was added. The absorbance was read at 450 nm with an ELISA plate reader (Model 550; Bio-Rad).

2.7. Wound healing migration assay

HAECs were plated in 24-well plates (5×10^5 cells/well) in ECM and were cultured until the formation of the cell monolayers. Then the layers were scratched by manual scraping with a 20 μL micropipette tip before washing with PBS. The cells were then incubated with ECM containing 1% bovine serum only or respectively together with HDL, 4F, HDL + 4F, Cl-HDL, Cl-HDL + 4F, NO_2-HDL, or NO_2-HDL + 4F for 18 h (native HDL, Cl/NO_2-HDL at 100 μg/mL apoA-1 and 4F at 50 μg/mL concentration). Then the HAEC were fixed with methanol, stained with hematoxylin–eosin, and observed under an inverted microscope (Nikon, Japan). The cells that had migrated into the wound edge were photographed and quantified in 10 random high-power (100×) fields. Results were confirmed in at least three independent experiments.

2.8. Transwell migration assay

Apart from wound healing migration assay, quantitative migration assays with HAECs were performed using a modified Boyden chamber (Minicell; Millipore, USA) with 8.0 μm pore polycarbonate filter inserted in a 24-well plate. The lower chamber was filled with 600 μL of ECM and 5% bovine serum. HAECs (1×10^5 cells/well) in ECM and 1% bovine serum were plated into the upper chamber. HDL, 4F, HDL + 4F, Cl-HDL, Cl-HDL + 4F, NO_2-HDL, and NO_2-HDL + 4F were added to each well and incubated for 5 h (native HDL, Cl/NO_2-HDL at 100 μg/mL apoA-1 and 4F at 50 μg/mL concentration) respectively. Then all non-migrated cells were removed from the upper chamber of the transwell membrane with a cotton swab while migrated cells were fixed and stained with hematoxylin eosin stain. Migrated cells in 20 random high-power (100×) fields were photographed with an inverted microscope (Nikon, Japan) for each chamber.

2.9. Single cell migration assay

Single cell migration assay was performed as previously described [50]. Briefly, glass bottom culture dishes (Nest Biotechnology Co.) were first coated with 50 μg/mL of fibronectin (FN, Santa Cruz Biotechnology, Inc.) at 37 °C for 1 h and thoroughly washed with distilled water. Cells were then seeded at 6×10^3 cells per cm^2 for 8–12 h. Then cells were labeled with 1 μM 5-chloromethylfluorescein diacetate (CellTracker green CMFDA from Molecular Probes, Invitrogen) in serum-free medium for 30 min. After washing with PBS, the cells were incubated with ECM containing either 1% bovine serum only or in combination with HDL, 4F, HDL + 4F, Cl-HDL, Cl-HDL + 4F, NO_2-HDL, or NO_2-HDL + 4F for 6 h (native HDL, Cl/NO_2-HDL at 100 μg/mL apoA-1 and 4F at 50 μg/mL concentration). Time-lapse microscopy was performed afterwards on fluorescent Nikkon A1R microscope (10 × objective) equipped with the heated stage and environmental chamber. Cell speed was measured with ImageJ using the Manual Tracking plugin (http://rsbweb.nih.gov/ij/plugins/track/track.html) and plotted with GraphPad Prism.

2.10. Lamellipodia formation

Sterilized coverslips were placed in a 24-well plate and HAECs were seeded on the coverslips. After 12 h, control (PBS), HDL, 4F, HDL + 4F, Cl-HDL, Cl-HDL + 4F, NO_2-HDL, and NO_2-HDL + 4F were added to each well respectively (native HDL, Cl/NO_2-HDL at 100 μg/mL apoA-1 and 4F at 50 μg/mL concentration). After 15 min the medium was removed, and the cells were fixed with methanol, stained with rhodamine phalloidin (Cytoskeleton, USA) and cell nuclei were counterstained with DAPI (Beyotime, China) according to the manufacturer's protocol. Then the cells were imaged using a laser scanning confocal microscope (Leica TCS SP5, Germany). Data are representative of three independent experiments.

2.11. Western blot

eNOS, Akt phosphorylation, eNOS, Akt, and SR-B1 were analyzed by Western blot. HAEC were cultured in 12-well plates and starved overnight. Then cells were treated with native HDL, 4F, HDL + 4F, Cl-HDL, Cl-HDL + 4F, NO_2-HDL, and NO_2-HDL + 4F (native HDL, Cl/NO_2-HDL at 100 μg/mL apoA-1 and 4F at 50 μg/mL concentration) for various times. Afterwards, cells were harvested and lysed in a mixture containing radioimmunoprecipitation assay buffer (Beijing Applygen Technologies Inc., China) in the presence of protease and phosphatase inhibitors (Applygen Technologies Inc., China). Cell debris was removed by centrifugation at 12,000 rpm for 20 min, and the protein concentration was determined using Coomassie brilliant blue method. Then cell lysates (100 μg protein per lane) were subjected to electrophoresis on 10% sodium dodecyl sulfate–polyacrylamide gels and

transferred onto nitrocellulose membranes (Pall Corp., USA) according to standard procedures. The membranes were blocked for 2 h with 5% nonfat milk. Membranes were incubated with each primary antibody (1:500–1:2000 dilution) overnight at 4 °C followed by the appropriate horseradish peroxidase (HRP)-conjugated secondary antibody (1:1000 dilution). Antibody binding was detected using the SuperSignal West Pico Kit (Pierce, USA) according to the manufacturer's instructions. Antibodies to p-eNOS (S1177; cat.no 9571S), p-eNOS (Thr495; cat.no 9574S), eNOS (cat.no 9572S), AKT (cat. no. 9272S) were purchased from Cell Signaling Technology. p-AKT (S473; cat.no. 2118-1), SR-B1(cat. no. ab52629), Actin (cat. no. 1844-1) were purchased from Abcam.

2.12. Measurement of intracellular ROS, plasma lysoPC and urine 8-isoprostane

Intracellular ROS levels were detected using the oxidant-sensitive probe 2′,7′-dichlorofluorescein diacetate. HAECs were planted on 12 well plate with endothelial cell medium and 5% fetal bovine serum at a density of 2×10^5 cells/mL for 6 h. Then cells were treated with 4F (50 μg/mL) for 8 h. Subsequently, cells were washed twice with PBS and incubated with 10 μM of 2′,7′-dichlorofluorescein diacetate for 30 min. DCF fluorescence was detected at 480 nm with a Leica DM IRB inverted fluorescence microscope. 6 randomly selected locations were captured in each well for analysis. Mice plasma was collected until the mice was sacrificed at selected time point. Plasma lysoPC concentration was determined by an enzymatic method (Cosmo Bio Inc. USA). Urine 8-isoprostane was measured with an enzyme linked immunosorbent assay kit (Cayman Chemical Co. USA).

2.13. siRNA Knockdown of SR-B1

SR-B1 siRNA transfection was performed. SR-B1 siRNAs (sense: 5′-GGACAA GUUCGGAUUAUUUdTdT-3′; antisense: 5′-AAAUAAUCCGAACUUGUCCTdTd-3′) were synthesized by Shanghai GenePharma Co (Shanghai, China). HAECs were plated in 6-well plates. After 30–50% confluence, HAECs were transfected with 100 nM of SR-B1 siRNA or scrambled siRNA in Opti-MEM with lipofectamine RNAiMIX reagent (Invitrogen) for 4–5 h, And then, incubated in ECM with 2.5% FBS for 48 h followed by further treatment with HDL for 12 h. The cells were then used for further experiments.

2.14. NO detection

HAECs were plated in 12-well plates (2×10^5 cells/well) in ECM with 5% bovine serum and cultured until 90% confluence. Then cells were treated with HDL, 4F, HDL + 4F, Cl-HDL, Cl-HDL + 4F, NO_2-HDL, and NO_2-HDL + 4F (normal HDL, Cl/NO_2-HDL at 100 μg/mL apoA-1 and 4F at 50 μg/mL concentration) for 15 min. Afterwards, cell media were collected and cell debris was removed by centrifugation at 12,000 rpm for 20 min. Cell protein was harvested and concentration was determined using coomassie brilliant blue method. Supernatant nitrites and nitrates were measured as surrogates for NO levels, and determined by a fluorometric method (NO assay kit; Beyotime Biotechnology Inc., China) and standardized to the protein concentration.

2.15. Electric injury model and Immunohistochemistry

Carotid artery electric injury was performed as described previously [20,51]. Mice were anesthetized by inhalation of 2.5% isoflurane. Surgery was carried out on the left common carotid artery with a dissection microscope (CNMICRO, SMZ-B2). The neck skin was bluntly dissected after an anterior incision of the neck, and the left common carotid artery was exposed. The electric injury was applied to the distal part of the common carotid artery. The carotid artery was injured by two alligator clips with copper tips (1 mm wide) positioned around the artery without applying mechanical pressure to the vessel to standardize the temperature increase in the vessel wall. An electric current of 0.8 mA was applied for 2 s to each millimeter of carotid artery over a total length of exactly 4 mm with the use of a plastic size marker parallel to the carotid artery. HDL, 4F, HDL + 4F, Cl-HDL, Cl-HDL + 4F, NO_2-HDL, and NO_2-HDL + 4F (native HDL, Cl/NO_2-HDL at 100 μg/mL apoA-1 and 4F at 50 μg/mL concentration) in a total volume of 200 μL were respectively injected *via* the tail vein after carotid artery injury every other day. The same volume of PBS (control) was injected into control mice. At selected times (1, 3, and 7 days) after injury, the mice were sacrificed by cervical dislocation then perfused with 25 mL of saline and then 4% phosphate-buffered formalin (pH 7.0). The injured vessel segments were dissected and fixed in 4% formalin for 8 h, and then transferred to cold PBS containing 20% sucrose overnight. Afterwards, the vessel segments were embedded in OCT (optimal cutting temperature) compound (Tissue-Tek; USA), snap-frozen in liquid nitrogen, and stored at − 80 °C for further use. 7 μm-thickness sections were cut at every 500-mm-spaced interval of the injured carotid artery (4 mm), and sections from the middle of the segments were stained with hematoxylin eosin or the goat antiserum for immunohistochemistry as described below. Endothelial cells were immunostained using a rabbit anti-CD31 antibody against mouse (Zhongshan Goldenbridge Biotechnology Co. Ltd.) and a mouse anti-PCNA (proliferating cell nuclear antigen) antibody (Zhongshan Goldenbridge Biotechnology Co. Ltd.). The cells were then stained with by HRP-conjugated anti-rabbit IgG polymer and HRP-conjugated anti-mouse IgG polymer (Zhongshan Goldenbridge Biotechnology) respectively, and finally coloration with 3,3-diaminobenzidin (DAB). Representative histological photomicrographs are shown (200×).

2.16. Statistical analysis

All experiments were performed multiple observations of biological and technical replicates. Results were presented as the mean ± SEM or as the percentage change compared to control. The non-parametric analyses were used in the data analysis with GraphPad Prism software (GraphPad Prism Software version 7, USA) and values were considered significant at $P < 0.05$.

3. Results

3.1. 4F at optimal concentration promoted proliferation of Human Aorta Endothelial cells (HAEC)

We first examined the effect of various concentrations of 4F on the proliferation of HAEC in culture. HAECs were incubated with increasing concentration of 4F (0–100 μg/mL), and 4F improved HAEC proliferation with a concentration-dependent effect and at a peak maximum of 21.0% at 50 μg/mL (Fig. 1A). Thus, we chose working concentration of 4F at 50 μg/mL for all the following experiments.

3.2. 4F restored the decreased ability of Cl/NO_2-HDL in promoting proliferation of HAECs mediated by SR-B1

To determine the effects of different treatments on HAEC proliferation, we used the BrdU cell proliferation assay. Exposure of cells to HDL, 4F, and HDL + 4F significantly stimulated HAEC proliferation compared with control (PBS) by 32.5%, 31.8% and 33.7% respectively. However, chlorinated HDL (Cl-HDL) and nitrated HDL (NO_2-HDL) dramatically diminished proliferation compared with HDL by 19.9% and 24.4% respectively (Fig. 1B). And, the reduced capability of Cl-HDL and NO_2-HDL in promoting HAEC proliferation could be reversed by adding 4F at 50 μg/mL concentration. When HAEC are treated with Cl-HDL + 4F and NO_2-HDL + 4F, HAEC proliferation was increased by 13.6% and 18.2% compared with Cl-HDL and NO_2-HDL treatment

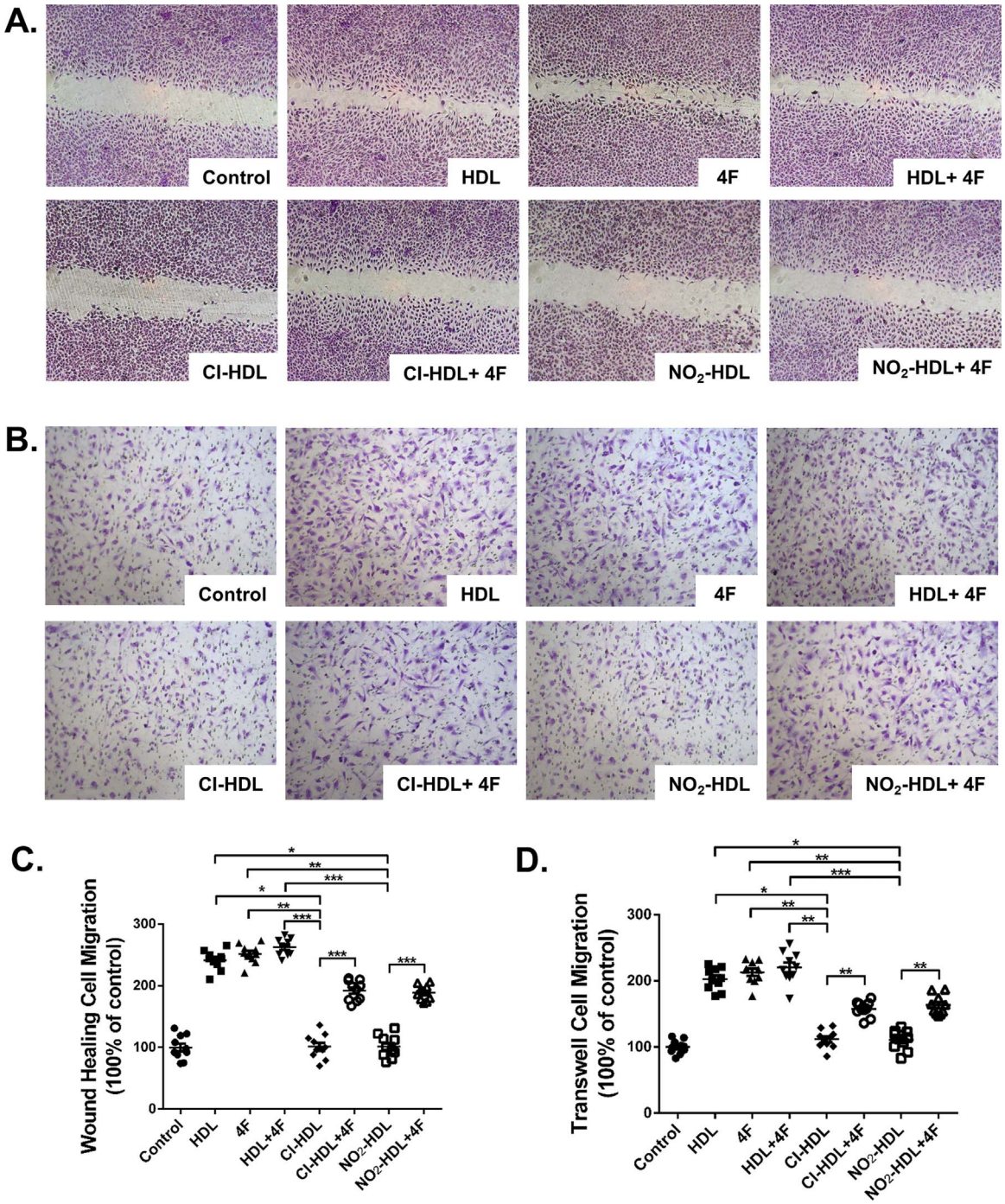

Fig. 2. Effects of 4F on HAECs migration and Cl/NO_2-HDL function. Monolayer HAECs were wounded by manual scraping and were incubated with native HDL, Cl/NO_2-HDL at 100 μg/mL apoA-1 or 4F at 50 μg/mL concentration for 18 h. Migrated cells were photographed and counted in 10 random high-power (original magnification 100×) fields. (B) HAECs were treated with native HDL, Cl/NO_2-HDL at 100 μg/mL apoA-1 or 4F at 50 μg/mL concentration in the upper chamber for 5 h. Migrated cells in the transwell assay were photographed and counted in 10 random high-power (original magnification 100×) fields. (C) Quantification of wound-healing cell migration. (D) Migrated cells were counted in 10 random high-power (100×) fields. The experiments have six independent biological replicates and every replicate have three technical replicates.

alone respectively (Fig. 1B).

We then used aortic endothelial cells of SR-BI $^{(+/+)}$ mice and SR-BI $^{(-/-)}$ mice to determine the effect of 4F on endothelial cell proliferation. Interestingly, similar results were observed in SR-BI $^{(+/+)}$ aortic endothelial cells (Fig. 1C) while no difference in cell proliferation was observed with SR-BI$^{(-/-)}$ aortic endothelial cells (Fig. 1D), suggesting that 4F mediated endothelial proliferation through SR-B1. Use of SR-B1 siRNA with scrambled siRNA as control revealed that SR-B1 siRNA treated cells do not show the cell proliferation caused by 4F. This confirms that 4F acts *via* the SR-B1 pathway (1E, Supplementary Fig. 2). Fig. 1E to G reveal the levels of oxidation in tryptophan, methionine, and tyrosine various amino acid residues of HDL are elevated in Cl/NO_2-HDL using mass spectrometry.

3.3. 4F promotes migration of HAECs and overcomes impaired function of Cl/NO_2-HDL in HAEC migration

As shown in Fig. 2A and C, HDL, 4F and HDL + 4F increased the migration of HAECs into the wound area compared with control by 135.0%, 151.0% and 164.0% respectively while both Cl-HDL and NO_2-

HDL dramatically diminished the migration compared with HDL by 59.1%. 4F improved the diminished ability of Cl-HDL and NO_2-HDL in promoting HAEC migration. Cl-HDL + 4F and NO_2-HDL + 4F promote cell migration 51.8% and 66.7% over that with Cl-HDL and NO_2-HDL treatment alone respectively (Fig. 2A, C). LDL and HDL isolated from cardiovascular patients were also used as a control while VEGF as a positive control (Supplemental Figure 1).

To confirm these effects of 4F on endothelial cell migration, we incubated HAECs for 5 h in transwell plates with the various treatment conditions. The results were in agreement with the wound healing experiments (Fig. 2B). Briefly, 4F increased HAEC migration to 117.0% of the control value and 4F treatment improved Cl-HDL and NO_2-HDL mediated HAEC migration by 37.7% and 47.3% respectively (Fig. 2D).

To get a more specific cell migration data and to exclude any possible artifacts caused by cell proliferation variations, we performed the single cell migration assay. Cell tracker dye labeled HUVECs have plated on glass bottom culture dishes coated with 50 μg/mL of fibronectin, followed by treatments with various factors. Time-lapse microscopy was performed to monitor single cell migration, and cell speed was quantified by tracking individual cells from the time-lapse movies. We observed a 66.7% cell speed increase in the 4F treatment group *versus* control. We also noticed that 4F treatment rescued the ability of Cl-HDL and NO2-HDL in promoting cell migration (by 120.4% and 137.9% respectively) (Fig. 3, Movie S1).

Supplementary material related to this article can be found online at http://dx.doi.org/10.1016/j.redox.2017.11.027.

3.4. 4F stimulates lamellipodia formation in HAECs and compensates for the impaired function of Cl/NO_2-HDL in this process

To explore how different treatments can affect endothelial cell migration, we tested the initial effects of these treatments on the actin cytoskeleton. Lamellipodia formation is an indicator of actin polymerization and suggests active cell migration. Fully adherent and confluent HAECs were treated with native HDL or Cl/NO_2-HDL at 100 μg/mL, apoA-1 or 4F at 50 μg/m/L for 15 min (Fig. 4A). HDL, 4F and HDL + 4F substantially induced more lamellipodia per cell than control value by 2.9-fold, 2.6-fold and 2.7-fold respectively (Fig. 4C). Cl-HDL and NO_2-HDL effects were decreased (61.7% and 67.6% respectively compared with native HDL) less compared with native HDL (Fig. 4B). Nevertheless, by adding 4F in Cl-HDL and NO_2-HDL treatment, the formation of lamellipodia in HAECs increased to 89.3% and 61.7% respectively, confirming that 4F can contribute to cell migration and lamellipodia formation, as well as reverse the impaired function of Cl/NO_2-HDL. HUVECs appeared similar lamellipodia formation with 4F and Cl/NO_2-HDL treatments (Fig. 4B, D).

3.5. 4F activates eNOS, Akt phosphorylation and diminishes oxidative stress in endothelial cells

eNOS and Akt phosphorylation are involved in HDL mediated endothelial cell migration and proliferation [18,52,53]. We have previously demonstrated the role of Cl-HDL and NO_2-HDL in Akt phosphorylation on cell migration and proliferation [20]. We hypothesized that 4F exerted a similar influence on the eNOS and Akt phosphorylation. HAECs were incubated under various conditions and time periods. eNOS phosphorylation was increased after 15 min of 4F treatment (Fig. 5A, B and C). It was shown that eNOS phosphorylation of HDL, 4F, and HDL + 4F was increased 1.7-fold, 1.72-fold and 1.8-fold compared with control respectively. However, Cl-HDL and NO_2-HDL reduced phosphorylation of eNOS by 65.9% and 78.9% respectively while 4F can dramatically restore their function to an increase of 134.1% and 157.9% (Fig. 5A and B).

Similar results were observed in Akt phosphorylation. HDL, 4F and HDL + 4F stimulated 1.9-fold, 1.8-fold and 1.7-fold more phosphorylation level than control. Comparing with HDL, Cl-HDL and NO_2-HDL had

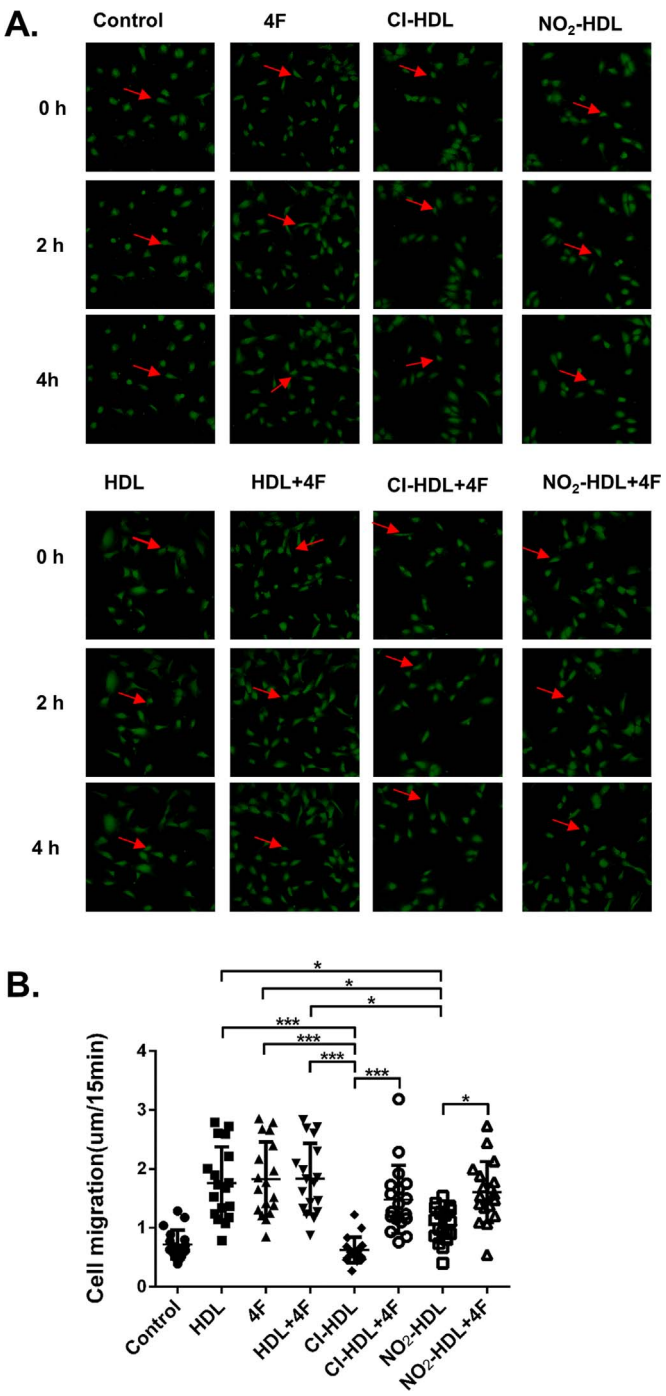

Fig. 3. HDL and 4F promote HUVECs directional migration. (A) HUVECs were plated on FN-coated glass bottom culture dishes and labeled with 1 μM, 5-chloromethylfluorescein diacetate. After cells were incubated with HDL, Cl/NO_2-HDL at 100 μg/mL apoA-1 and/or 4F at 50 μg/mL concentration for 6 h, time-lapse microscopy was performed on a fluorescent microscope (10× objective) with Nikon BioStation IM (10× objective). The red arrow follows the labeled cell across various time points. (B) Cell speed was measured in 20 random fields with ImageJ using the Manual Tracking plug-in. Cells migration into the gaps were quantified. Videos were shown in supplemental movie S1. These experiments have three independent biological replicates and HUVECs were isolated from three fresh cords and passages 2–5 was used.

reduced ability to activate Akt phosphorylation at 46.1% and 54.5% respectively, which can also be reversed by 4F to 36.4% and 41.7% increase relatively (Fig. 5A and D).

We measured the nitrite and nitrate content as surrogates of nitric oxide (NO) in HAEC treated with native HDL, Cl/NO_2-HDL at 100 μg/mL apoA-1 or 4F at 50 μg/mL concentration for 15 min showing the

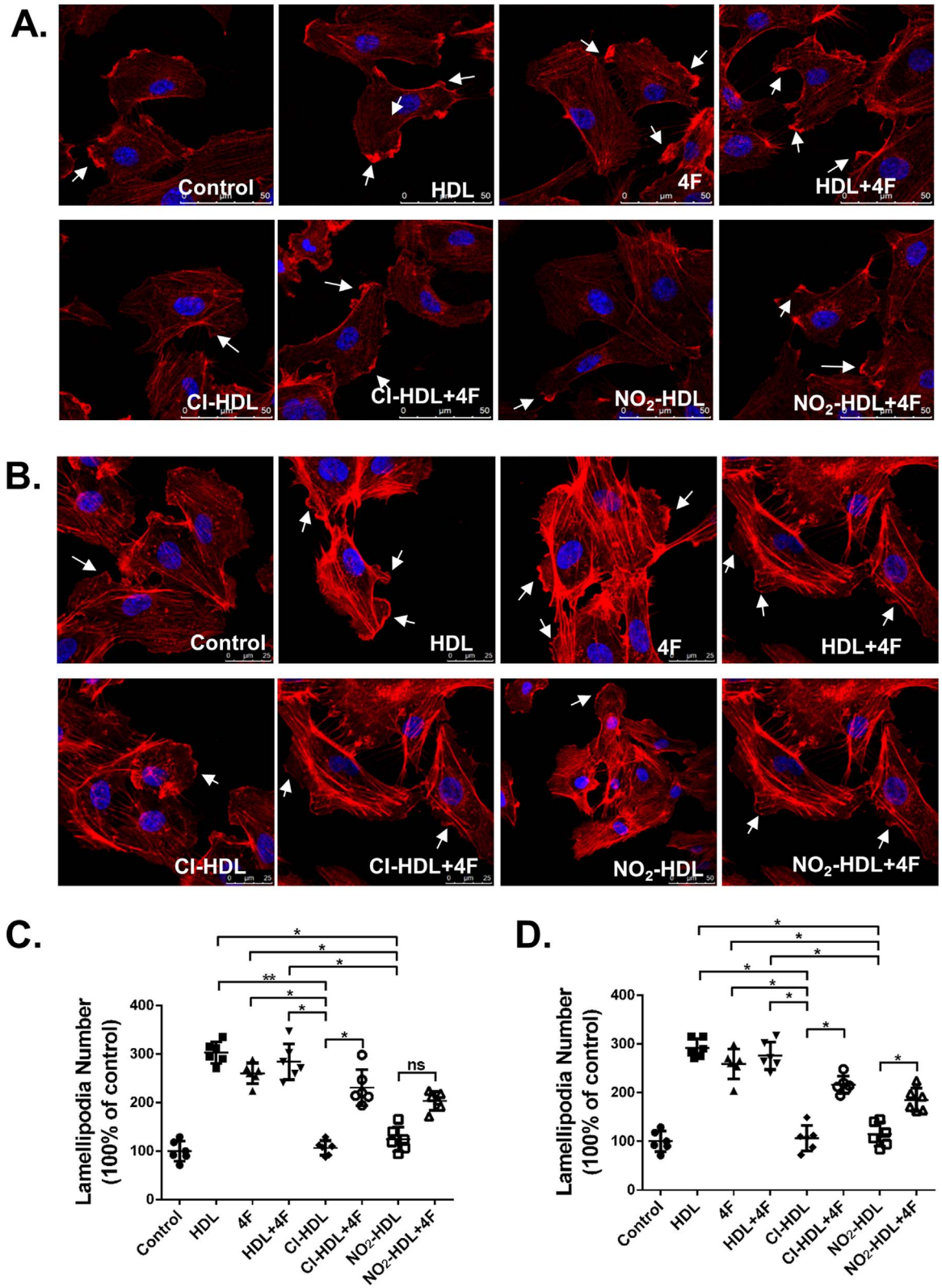

Fig. 4. Effects of 4F on the formation of lamellipodia in HUVECs and HAECs. HAECs(A) and HUVECs(B) were treated with native HDL, Cl/NO_2-HDL at 100 μg/mL apoA-1 and/or 4F at 50 μg/mL concentration for 15 min, and confocal images of lamellipodia in HUVECs are shown. HUVECs were stained with rhodamine phalloidin (red) and DAPI (blue). HAEC (C) and HUVEC (D) migrated cells were counted in 15 random high-power (200×) fields under varied conditions. The experiments were performed as six independent biological replicates and every replicate have three technical replicates.

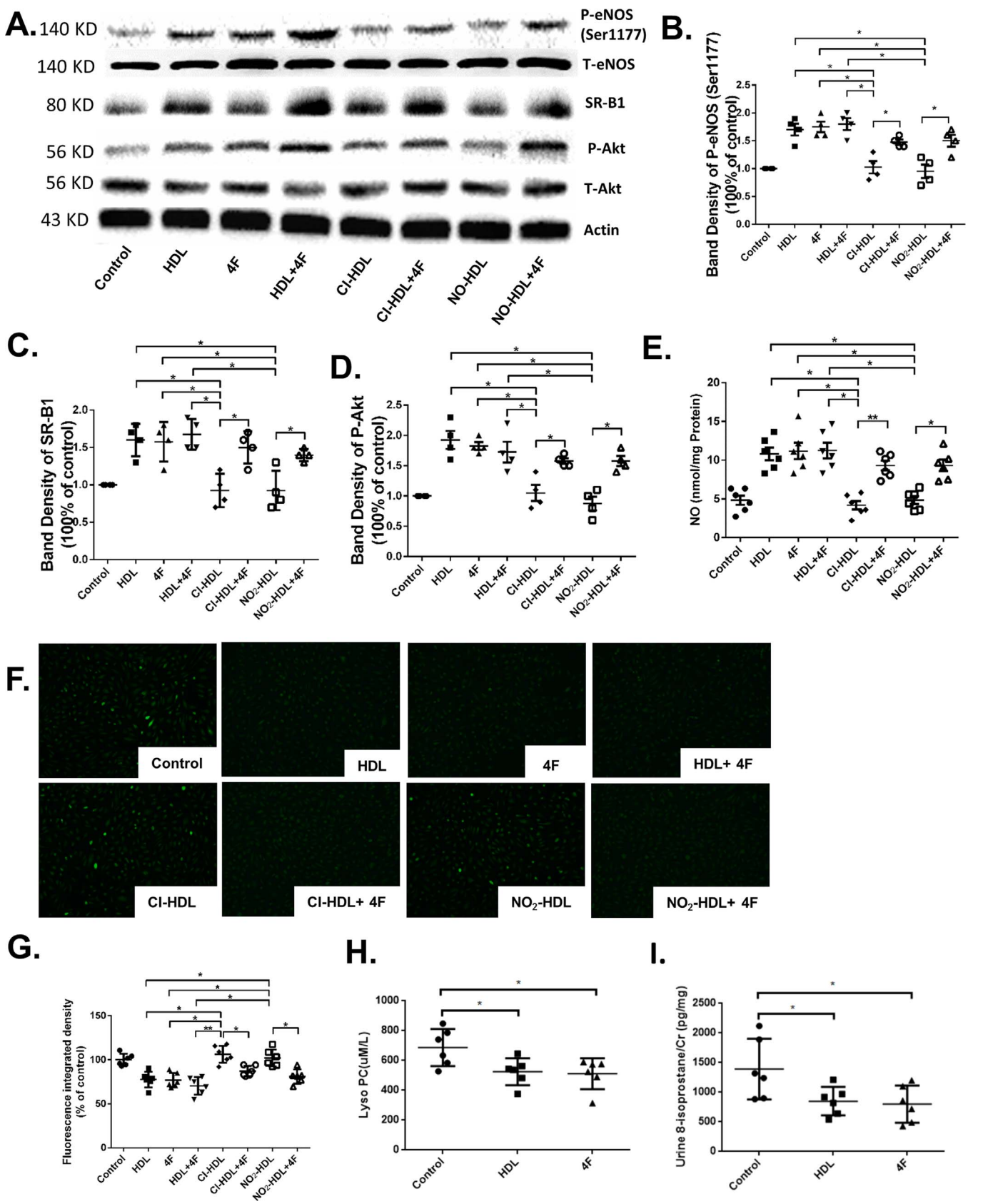

(caption on next page)

Fig. 5. HDL and 4F exert effects through activating eNOS, Akt phosphorylation, SR-B1 expression, and diminishing reactive oxygen stress. HAECs were treated with native HDL, Cl/NO_2-HDL at 100 μg/mL apoA-1 or 4F at 50 μg/mL concentration for 15 min. Cell lysates were analyzed by Western blotting using anti-phospho- Akt (Ser473) antibody, anti-phospho- eNOS (S1177) antibody, anti-total-Akt antibody, and anti-total-eNOS antibody. (B) Densitometry of phospho-eNOS bands was normalized to the total-eNOS bands. (C) Densitometry of SR-B1 bands was normalized to actin bands. (D) Densitometry of phospho-Akt bands was normalized to the total-Akt bands. (E) Nitric oxide (NO) determination in human aortic endothelial cells (HAEC) treated with native HDL, Cl/NO_2-HDL at 100 μg/mL apoA-1 or 4F at 50 μg/mL concentration for 15 min (F) Intracellular ROS levels were detected using the oxidant-sensitive probe 2′,7′-dichlorofluorescein diacetate in HAECs treated with 4F (50 μg/mL) for 8 h. 6 randomly selected locations were captured in each well for analysis. (G) Fluorescence integrated density of intracellular ROS of HAECs was quantified using imageJ. (H) Plasma lysoPC of WT mice treated with control, HDL and 4F were measured. (I) Urine 8-isoprostane of WT mice treated with control, HDL and 4F were measured. These experiments had four independent biological replicates and every group has 6–8 mice.

HDL and 4F increased NO production and that Cl-HDL and NO_2-HDL decrease NO production that was improved with 4F treatment (Fig. 5E). Reactive oxygen species (ROS) formation was measured in cells treated with 4 F/ox-HDL *in vitro* as showen in Fig. 5F. Plasma lysoPC (Fig. 5H) and urine 8-isoprostane (Fig. 5I) in electric injury mice treated with 4F were measured. The data demonstrated HDL, 4F and HDL + 4F inhibited the production of ROS compared with control while both Cl-HDL and NO_2-HDL dramatically diminished the protection effects compared with HDL *in vitro*. Treatment with 4F significantly lower lysoPC and 8-isoprostane levels compared with PBS group *in vivo*.

3.6. 4F promotes cell proliferation and reendothelialization in an in vivo model of endothelial injury

We tested our hypothesis that 4F mediates endothelial repair and re-endothelialization through the neointima formation process in a mouse model with electric-induced carotid injury [20]. The injury destroyed all medial smooth muscle cells and denuded all the intact endothelium in the injured segment. Endothelial cell marker CD31 (Fig. 6A and C) and standard hematoxylin eosin (Fig. 6B and D) staining revealed the gradual process of re-endothelialization, which is characterized by re-population of the media, and accumulation, proliferation and migration of endothelial cell within the neointima of smooth muscle cells originating from the non-injured borders. On day 1 after electric injury, no noticeable difference was observed between different treatment groups. From day 3 to day 7, it was demonstrated that the neointima was restored gradually at a different rate depending on various treatments. As shown in Fig. 6B, HDL, 4F, and HDL + 4F promoted faster re-endothelialization in contrast to Cl-HDL and NO_2-HDL while the impaired function of Cl/NO_2-HDL can be improved in an especially potent way by adding 4F treatment.

PCNA is a nuclear factor involved in DNA replication and repairing of proliferating cells. Cell proliferation was identified and evaluated by immunostaining for PCNA [20]. As shown in Fig. 7, treatment with HDL, 4F and HDL + 4F induced early endothelial cell proliferation within the neointima50.0%, 39.6% and 54.2% more than control on day 3. By day 7, 4F treated intima was distinguishable and recovered more thoroughly than others. However, weak strength and poor capability in stimulating endothelial cell proliferation were observed in Cl-HDL (52.8% decrease on day 3% and 74.1% on day 7) and NO_2-HDL (52.8% decrease on day 3% and 62.6% on day 7) in comparison with HDL. The diminished capability can be compensated by 4F (44.1% and 41.2% increase on day 3 for Cl-HDL and NO_2-HDL respectively; 48.2% and 37.4% increase on day 7 for Cl-HDL and NO_2-HDL respectively), indicating the restoration effect for Cl/NO_2-HDL was also a time-dependent process. The immunostaining was repeated in SR-$B1^{(-/-)}$ mice to demonstrate the lack of impact of 4F in these mice, thus proving that 4F action is related to the SR-B1 mechanism as seen in Supplemental Figure 2.

4. Discussion

Our study demonstrates that apoA-1 mimetic 4F promotes endothelial repair and restores the re-endothelialization impaired by the presence of oxidized HDL. These results are consistent with our previous work, and confirms that MPO catalyzed nitration and chlorination of HDL impairs its ability to induce proliferation and migration (Figs. 1–7). Directional migration assays that measure cell mobility using single-cell tracking demonstrate the effects of 4F on endothelial cell migration and re-endothelialization that are also supported by wound healing and transwell assays. In an *in vivo* model of endothelial injury, 4F appears to act through an SR-B1 related mechanism and phosphorylates eNOS and Akt. More importantly, the data reported herein indicate that apoA-1 mimetic peptide 4F can promote endothelial repairing and restore the impaired function of Cl/NO_2-HDL in re-endothelialization. Our data provided potential therapeutic targets for ameliorating the impaired effects of Cl/NO_2-HDL in cardiovascular diseases.

We have demonstrated in previous studies, that the oxidized HDL in diabetic patients downregulates SR-BI expression and the downstream phosphorylation of Akt influences endothelial proliferation and migration [21]. Similarly, HDL modified by the specific action of MPO is dysfunctional in promoting endothelial repair and proliferation by down regulating Akt and ERK1/2 phosphorylation [20]. Our study confirms this fact and demonstrates the ability of 4F to negate the action of Cl/NO_2-HDL by in promoting endothelial repair and re-endothelialization. 4F improves proliferation of HAECs, and SR-B1 mediates this action. SR-B1 expression, Akt phosphorylation and eNOS phosphorylation are upregulated with 4F treatment. The cell proliferation in endothelial repair was increased in a time-dependent manner in the presence of HDL or 4F in an *in vivo* model of electric induced carotid injury showing the evident influence of 4F in endothelial repair.

Heme enzyme MPO is bound to apoA-1 on residues A_{190}-L_{203}, in close spatial proximity to potential sites of MPO specific oxidative modifications through nitration (Tyr18, Tyr100 and Tyr192) and chlorination (Tyr192) in the pro-inflammatory environment of human atherosclerotic plaque [20,28,48,54]. Cl/NO_2-HDL is dysfunctional in repairing endothelium and in exerting other anti-atherosclerotic effects predominantly due to alterations of apoA-1 class A amphipathic helical structure by MPO [55]. The helical structure of apoA-1 which is vital for its physical-chemical and biological properties undergoes conformational change under the action of MPO. It results in impaired hydrophobic face-lipid acyl chain interaction activities when translocated in an aqueous environment. 4F did not affect MPO levels but reduced MPO association with apoA-1 occurring in a decreased 3-nitrotyrosine concentration of apoA-1 [56]. ApoA-1 mimetic peptide 4F has distinct differences compared to native apoA-1 in that in pathological conditions, and MPO released by activated leukocytes catalyzes the oxidation of the sole tryptophan residue in 4F in both lipid-free and lipid-bound states. However, unlike Cl/NO_2-HDL, 4F preserves its biological function in mediating lipid binding and ABCA1-dependent cholesterol efflux despite the oxidative modification [57]. Tryptophan residues have a unique transmembrane distribution pattern close to the polar-nonpolar interface of 4F, and MPO action does not significantly alter the helicity of 4F, and its lipid-associating capability. Lipid-associating capability is related to hydrophobic interaction or charged residue interaction with phospholipid head groups [57,58].

4F shares structural similarities with apoA-1, exerting comparable and even superior vascular protective properties. The 2-thiobarbituric acid (TBA) test is intrinsically nonspecific for malondialdehyde (MDA). Non-lipid-related materials as well as fatty peroxide-derived decomposition products other than MDA are TBA positive [59]. For the serious limitations the MDA method, lysophosphatidylcholine (lysoPC) was

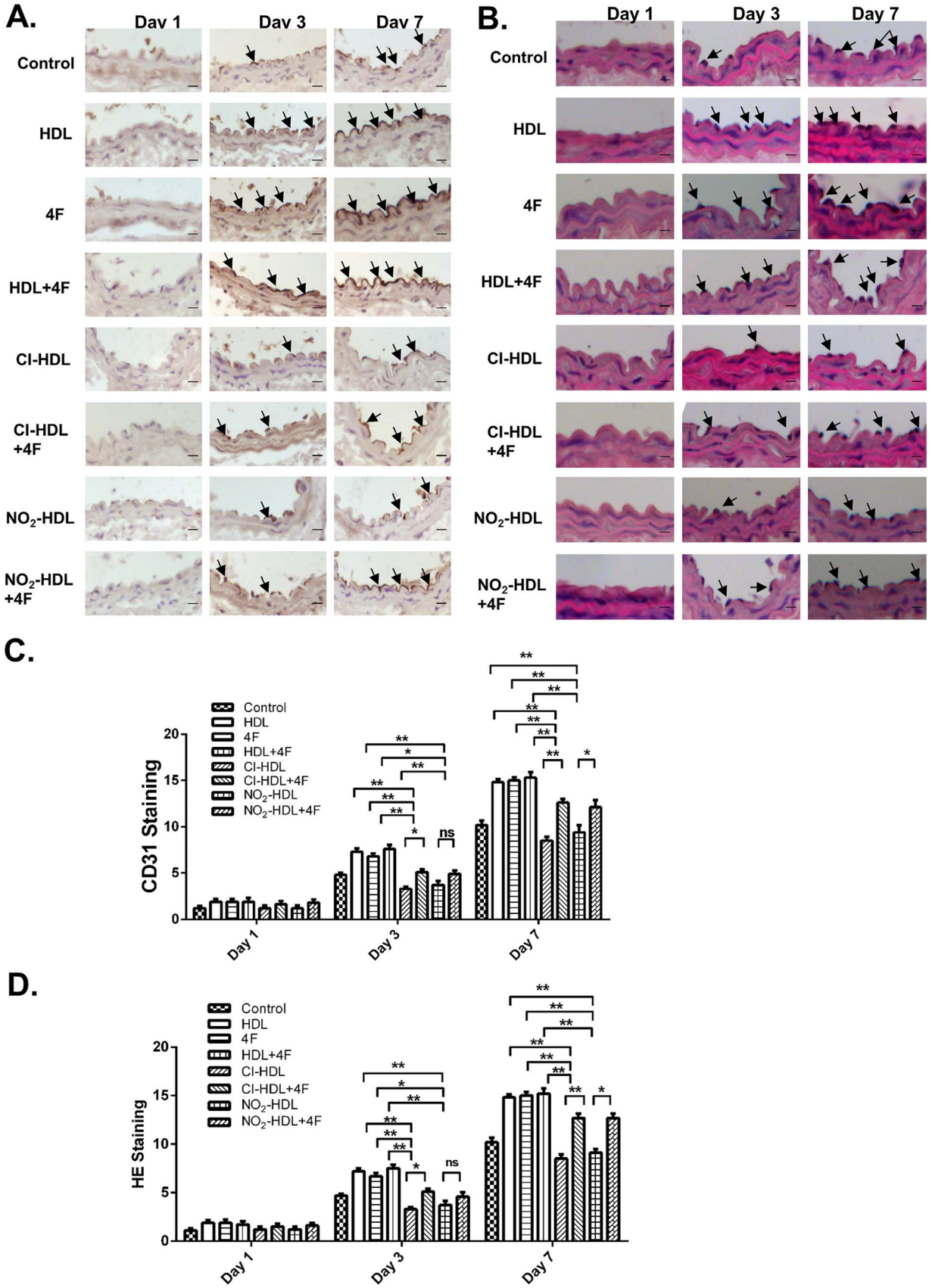

Fig. 6. Effects of 4F on re-endothelialization of the carotid artery of electric injury mice models and Cl/NO_2-HDL function. CD31-stained frozen sections of injured arteries at days 1, 3, and 7 treated with control (PBS), HDL, 4F, HDL + 4F, Cl-HDL, Cl-HDL + 4F, NO_2-HDL, or NO_2-HDL + 4F. Bar, 20 μm. (B) Representative photomicrographs of hematoxylin eosin (H&E)-stained sections of carotid arteries with various treatments. Bar, 20 μm. (C) Quantitative analysis of CD31-stained cells in neointima at 1 day, 3 days and 7 days respectively. (D) Quantitative analysis of HE-stained cells in neointima at 1 day, 3 days and 7 days respectively. The experiments had three independent biological replicates and every group had 6–8 mice. The space between groups is too close, and the figure was presented with bar graph rather than dot plots to display the data clearly.

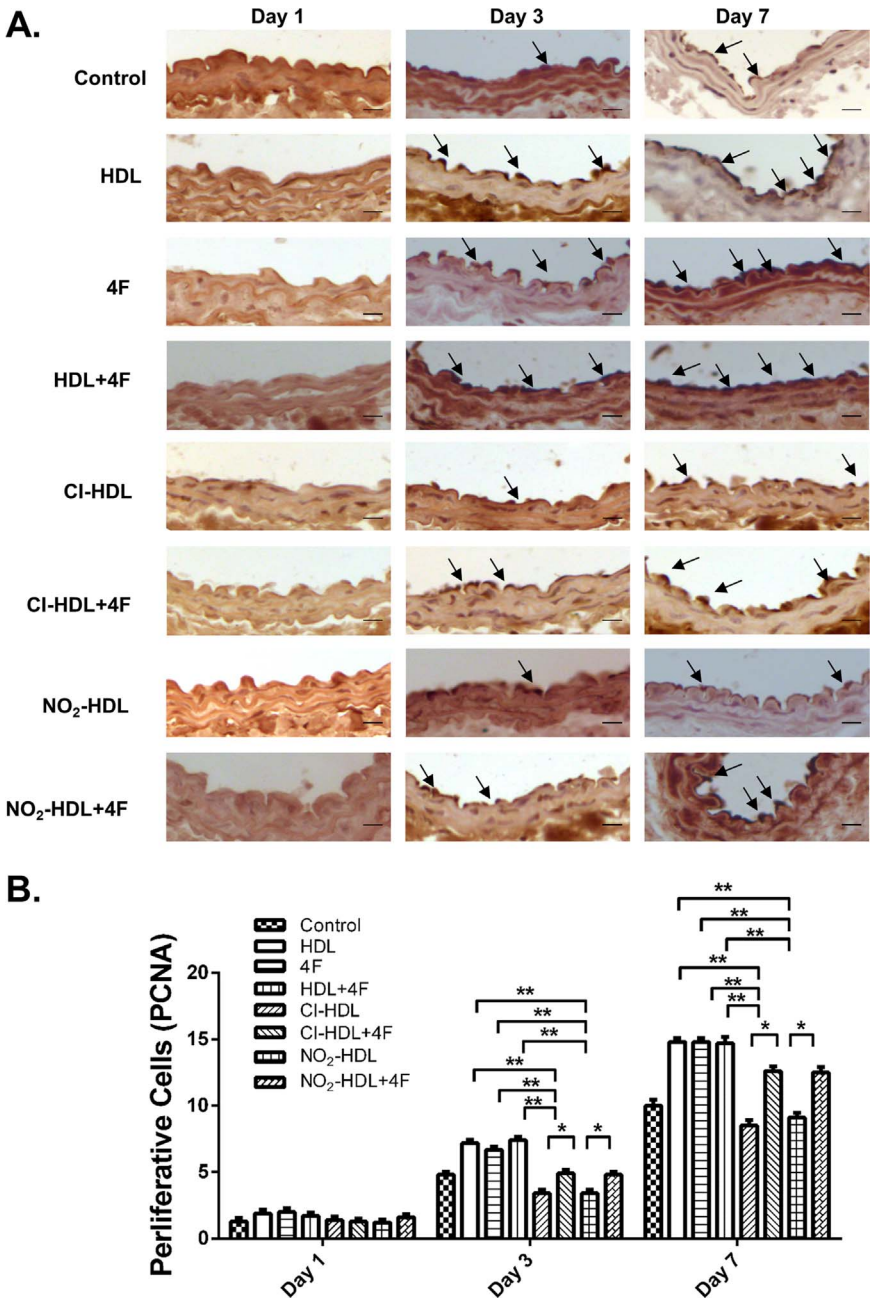

Fig. 7. Effects of 4F on cell proliferation in the intima of carotid artery of electric injury mice models and Cl/NO_2-HDL function. Representative photomicrographs show changes in cell proliferation in the intima of injured carotid arteries after treatment with control (PBS), HDL, 4 F, HDL + 4F, Cl-HDL, Cl-HDL + 4F, NO_2-HDL, or NO_2-HDL + 4F at days 1, 3, and 7. Cell proliferation was determined by immunohistochemistry with proliferative cell nuclear antigen (PCNA) labeling. Bar, 20 μm. (B) Quantitative analysis of cell proliferation by PCNA at neointima in 1 day, 3 days and 7 days respectively. The experiments had three independent biological replicates and every group had 6–8 mice. The space between groups is too close and the figure was presented with bar graph rather than dot plots to display the data clearly.

used as an oxidative stress marker. Oxidized LDL and lysoPC, the principal lysophospholipid in oxidized LDL, block EC migration *in vitro*. 4F rescues the effects of lysoPC on EC migration *in vitro* and *in vi*vo by improving endothelial healing of arterial injuries in hypercholesterolemic mice [60]. Oxidized phospholipids and oxidized fatty acids are reported to bind with much higher affinity to 4F than to apoA-1. Specifically, when the lipids are oxidized, the binding to apoA-1 reduced dramatically while the binding to 4F is markedly increased [46]. LysoPC has been shown to be a potent chemoattractant for T-cells and monocytes, which promotes endothelial dysfunction, induces the release of arachidonic acid, and induces apoptosis of endothelial and vascular smooth muscle cells [61]. Moreover, studies have shown that 4F decreases plasma lysoPC levels in hypercholesterolemic mice [62], and this has been attributed to the microdomains of 4F that interact with lipid membranes. It provides a thermodynamically favorable environment for binding more polar oxidized lipids, which makes it easier for 4F to sequestrate oxidized lipids from the aqueous environment [46,63]. Besides, 4F induces the expression of microRNA-193-3p (miR193) by suppressing the peroxisome proliferator-activated receptor/RXR-α signaling pathway and regulates lipoxygenases that form these oxidized lipids [17,40]. 4F protects HUVECs from oxidized LDL-induced injury by preventing the downregulation of pigment epithelium-derived factor expression [64].

One of the mechanisms by which oxidized LDL and lysoPC inhibit EC migration is through an increase in EC production of superoxide by NAD(P)H oxidase [65]. Rosenbaum et al. demonstrated that 4F decreased ROS, but 4F did not alter NAD(P)H oxidase activity. 4F might act as a scavenger of ROS or increase the activity of superoxide dismutase [60]. In our study, 4F does not cause change in oxidized LDL incorporation in vessel wall at seven days but reduces levels of oxidative stress, including cellular ROS, plasma lysoPC and urinary 8-isoprostane levels, which inversely correlate with endothelial healing. Limited studies have focused on the influence 4F on endothelial repair, and 4F increased eNOS related vasodilation in LDLr $^{(-/-)}$ mice [56]. In a

recent study in diabetic rats, daily 4F administration prevented loss of endothelial cells and promoted endothelial repair. 4F upregulates the eNOS/NO pathway and expression of heme oxygenase (HO)-1 demonstrating a protective and defensive phenotype, confirmed by simultaneous upregulation of CD31 + expression and thrombomodulin [66,67]. Both markers can improve endothelial function. Our study also shows evidence of the favorable role of 4F in endothelial proliferation and repair *via* an eNOS/Akt phosphorylation pathway.

4F interacts with HDL and incorporates into the HDL particles [68]. 4F particles, compared to reconstituted HDL and the apoA-1 particles, are 14- and 20-fold more efficient in delivering its cholesterol ester core respectively [69]. 4F can normalize the composition and function of the existing dysfunctional HDL through stimulating HDL remodeling and the formation of pre-β HDL which is considered to be the most active HDL fraction in promoting reverse cholesterol transport [45,70]. 4F reduces lipid rafts in macrophages to decrease the production of pro-inflammatory cytokines and chemokines [36,71]. 4F also binds with paraoxonase-1 (PON1) which forms a complex with MPO and enhances PON1 activity [72]. PON1 has been shown to foster systemic antioxidant effects, stimulate HDL-mediated eNOS-dependent NO production, and promote cholesterol efflux from cholesterol-laden macrophages [28,72,73]. 4F therapy has been thought to be a novel platform for PON-1 binding and enhancing its activity and stability. It further inhibits MPO activity and protects HDL from being oxidized [72].

Clinical trials have explored the safety, pharmacokinetics, and pharmacodynamics of oral apoA-1 mimetic peptide 4F in high-risk cardiovascular patients. Data from these studies indicate that 4F was most effective at preventing atherosclerosis when taken orally and processed in the digestive system [43]. 4F was administered orally at doses starting at 30 mg up to 500 mg, the higher doses significantly improved the HDL inflammatory index (HII; the ability of HDL to inhibit LDL-induced monocyte chemoattractant protein-1) [44]. Plasma native and oxidized apoA-1 levels were comparable at 8 h after subcutaneous injection, with oxidized apoA-1 declining at 24 h while native maintaining [74]. In our study, we found 4F administration *via* tail vein injection could stimulate EC proliferation in the intima of carotid artery and re-endothelialization which protected endothelial monolayer integrity in the early stage of atherosclerosis and recovered the impaired function of Cl/NO_2-HDL *in vitro* and *in vivo*. While there is a clear benefit in apoA-1 infusion therapy, the monetary cost of apoA-1 therapy would be immense. The use of peptide mimetic to improve HDL associated functions is a powerful tool, and this study demonstrates that 4F promotes endothelial cell proliferation and migration *in vivo* and *in vitro* and recovers impaired Cl/NO_2-HDL function in the early stage of atherosclerosis. These findings stress the potential therapeutic value of 4F in recovering the impaired function of MPO-oxidized HDL in cardiovascular diseases.

Funding

This work was supported by Grants 91639108, 81172500, 81322005, 81370235 and 81770272 from the National Natural Science Foundation of China. This project was also supported by Grant 2016YFC0903000 from Ministry of Science and Technology of China.

Conflict of interest

None declared.

Appendix A. Supporting information

Supplementary data associated with this article can be found in the online version at http://dx.doi.org/10.1016/j.redox.2017.11.027

References

[1] T. Gordon, W.P. Castelli, M.C. Hjortland, W.B. Kannel, T.R. Dawber, High density lipoprotein as a protective factor against coronary heart disease. The Framingham Study, Am. J. Med. 62 (1977) 707–714.
[2] N.J. Stone, J.G. Robinson, A.H. Lichtenstein, C.N. Bairey Merz, C.B. Blum, R.H. Eckel, A.C. Goldberg, D. Gordon, D. Levy, D.M. Lloyd-Jones, P. McBride, J.S. Schwartz, S.T. Shero, S.C. Smith Jr., K. Watson, P.W. Wilson, K.M. Eddleman, N.M. Jarrett, K. LaBresh, L. Nevo, J. Wnek, J.L. Anderson, J.L. Halperin, N.M. Albert, B. Bozkurt, R.G. Brindis, L.H. Curtis, D. DeMets, J.S. Hochman, R.J. Kovacs, E.M. Ohman, S.J. Pressler, F.W. Sellke, W.K. Shen, S.C. Smith Jr., G.F. Tomaselli, G. American College of Cardiology/American Heart Association Task Force on Practice, ACC/AHA guideline on the treatment of blood cholesterol to reduce atherosclerotic cardiovascular risk in adults: a report of the American College of Cardiology/American Heart Association Task Force on Practice Guidelines, Circulation 129 (2013) S1–S45 (2014).
[3] R.P. Choudhury, J.X. Rong, E. Trogan, V.I. Elmalem, H.M. Dansky, J.L. Breslow, J.L. Witztum, J.T. Fallon, E.A. Fisher, High-density lipoproteins retard the progression of atherosclerosis and favorably remodel lesions without suppressing indices of inflammation or oxidation, Arterioscler. Thromb. Vasc. Biol. 24 (2004) 1904–1909.
[4] J.E. Feig, J.X. Rong, R. Shamir, M. Sanson, Y. Vengrenyuk, J. Liu, K. Rayner, K. Moore, M. Garabedian, E.A. Fisher, HDL promotes rapid atherosclerosis regression in mice and alters inflammatory properties of plaque monocyte-derived cells, Proc. Natl. Acad. Sci. USA 108 (2011) 7166–7171.
[5] J.E. Feig, B. Hewing, J.D. Smith, S.L. Hazen, E.A. Fisher, High-density lipoprotein and atherosclerosis regression: evidence from preclinical and clinical studies, Circ. Res. 114 (2014) 205–213.
[6] S.J. Nicholls, E.M. Tuzcu, I. Sipahi, A.W. Grasso, P. Schoenhagen, T. Hu, K. Wolski, T. Crowe, M.Y. Desai, S.L. Hazen, S.R. Kapadia, S.E. Nissen, Statins, high-density lipoprotein cholesterol, and regression of coronary atherosclerosis, JAMA 297 (2007) 499–508.
[7] H. Dan, P. Bing, R. Hui, Z. Lemin, *Effects of Diabetic HDL* on Endothelial Cell Function, Cardiovasc. Hematol. Disord.-Drug Targets 14 (2014) 137–141.
[8] B.J. Van Lenten, S.Y. Hama, F.C. de Beer, D.M. Stafforini, T.M. McIntyre, S.M. Prescott, B.N. La Du, A.M. Fogelman, M. Navab, Anti-inflammatory HDL becomes pro-inflammatory during the acute phase response. Loss of protective effect of HDL against LDL oxidation in aortic wall cell cocultures, J. Clin. Investig. 96 (1995) 2758–2767.
[9] H. Zhang, M.P. Reilly, Anti-inflammatory effects of high-density lipoprotein through activating transcription factor 3: benefit beyond cholesterol transport-dependent processes, Arterioscler. Thromb. Vasc. Biol. 34 (2014) e11–e12.
[10] K.J. Moore, E.A. Fisher, High-density lipoproteins put out the fire, Cell Metab. 19 (2014) 175–176.
[11] A.J. Iqbal, T.J. Barrett, L. Taylor, E. McNeill, A. Manmadhan, C. Recio, A. Carmineri, M.H. Brodermann, G.E. White, D. Cooper, J.A. DiDonato, M. Zamanian-Daryoush, S.L. Hazen, K.M. Channon, D.R. Greaves, E.A. Fisher, Acute exposure to apolipoprotein A1 inhibits macrophage chemotaxis in vitro and monocyte recruitment in vivo, eLife (2016) 5.
[12] A. Kontush, M.J. Chapman, Antiatherogenic function of HDL particle subpopulations: focus on antioxidative activities, Curr. Opin. Lipidol. 21 (2010) 312–318.
[13] L. Camont, M. Lhomme, F. Rached, W. Le Goff, A. Negre-Salvayre, R. Salvayre, C. Calzada, M. Lagarde, M.J. Chapman, A. Kontush, Small, dense high-density lipoprotein-3 particles are enriched in negatively charged phospholipids: relevance to cellular cholesterol efflux, antioxidative, antithrombotic, anti-inflammatory, and antiapoptotic functionalities, Arterioscler. Thromb. Vasc. Biol. 33 (2013) 2715–2723.
[14] N. Terasaka, N. Wang, L. Yvan-Charvet, A.R. Tall, High-density lipoprotein protects macrophages from oxidized low-density lipoprotein-induced apoptosis by promoting efflux of 7-ketocholesterol via ABCG1, Proc. Natl. Acad. Sci. USA 104 (2007) 15093–15098.
[15] P.O. Bonetti, L.O. Lerman, A. Lerman, Endothelial dysfunction: a marker of atherosclerotic risk, Arterioscler. Thromb. Vasc. Biol. 23 (2003) 168–175.
[16] K.S. Cunningham, A.I. Gotlieb, The role of shear stress in the pathogenesis of atherosclerosis, Lab. Investig. 85 (2005) 9–23.
[17] R. Ross, The pathogenesis of atherosclerosis: a perspective for the 1990s, Nature 362 (1993) 801–809.
[18] D. Seetharam, C. Mineo, A.K. Gormley, L.L. Gibson, W. Vongpatanasin, K.L. Chambliss, L.D. Hahner, M.L. Cummings, R.L. Kitchens, Y.L. Marcel, D.J. Rader, P.W. Shaul, High-density lipoprotein promotes endothelial cell migration and reendothelialization via scavenger receptor-B type I, Circ. Res. 98 (2006) 63–72.
[19] L.E. Spieker, I. Sudano, D. Hurlimann, P.G. Lerch, M.G. Lang, C. Binggeli, R. Corti, F. Ruschitzka, T.F. Luscher, G. Noll, High-density lipoprotein restores endothelial function in hypercholesterolemic men, Circulation 105 (2002) 1399–1402.
[20] B. Pan, B. Yu, H. Ren, B. Willard, L. Pan, L. Zu, X. Shen, Y. Ma, X. Li, C. Niu, J. Kong, S. Kang, Y. Eugene Chen, S. Pennathur, L. Zheng, High-density lipoprotein nitration and chlorination catalyzed by myeloperoxidase impair its effect of promoting endothelial repair, Free Radic. Biol. Med. 60 (2013) 272–281.
[21] B. Pan, Y. Ma, H. Ren, Y. He, Y. Wang, X. Lv, D. Liu, L. Ji, B. Yu, Y. Wang, Y.E. Chen, S. Pennathur, J.D. Smith, G. Liu, L. Zheng, Diabetic HDL is dysfunctional in stimulating endothelial cell migration and proliferation due to down regulation of SR-BI expression, PLoS One 7 (2012) e48530.
[22] G. Giannotti, C. Doerries, P.S. Mocharla, M.F. Mueller, F.H. Bahlmann, T. Horvath, H. Jiang, S.A. Sorrentino, N. Steenken, C. Manes, M. Marzilli, K.L. Rudolph,

T.F. Luscher, H. Drexler, U. Landmesser, Impaired endothelial repair capacity of early endothelial progenitor cells in prehypertension: relation to endothelial dysfunction, Hypertension 55 (2010) 1389–1397.
[23] Y. Feng, F. Jacobs, E. Van Craeyveld, C. Brunaud, J. Snoeys, M. Tjwa, S. Van Linthout, B. De Geest, Human ApoA-I transfer attenuates transplant arteriosclerosis via enhanced incorporation of bone marrow-derived endothelial progenitor cells, Arterioscler. Thromb. Vasc. Biol. 28 (2008) 278–283.
[24] K. Mythreye, L.L. Satterwhite, W.S. Davidson, P.J. Goldschmidt-Clermont, ApoA-I induced CD31 in bone marrow-derived vascular progenitor cells increases adhesion: implications for vascular repair, Biochim. Biophys. Acta 1781 (2008) 703–709.
[25] V. Petoumenos, G. Nickenig, N. Werner, High-density lipoprotein exerts vasculoprotection via endothelial progenitor cells, J. Cell Mol. Med. 13 (2009) 4623–4635.
[26] V. Gonzalez-Pecchi, S. Valdes, V. Pons, P. Honorato, L.O. Martinez, L. Lamperti, C. Aguayo, C. Radojkovic, Apolipoprotein A-I enhances proliferation of human endothelial progenitor cells and promotes angiogenesis through the cell surface ATP synthase, Microvasc. Res. 98 (2015) 9–15.
[27] L. Zheng, B. Nukuna, M.L. Brennan, M. Sun, M. Goormastic, M. Settle, D. Schmitt, X. Fu, L. Thomson, P.L. Fox, H. Ischiropoulos, J.D. Smith, M. Kinter, S.L. Hazen, Apolipoprotein A-I is a selective target for myeloperoxidase-catalyzed oxidation and functional impairment in subjects with cardiovascular disease, J. Clin. Investig. 114 (2004) 529–541.
[28] Y. Huang, Z. Wu, M. Riwanto, S. Gao, B.S. Levison, X. Gu, X. Fu, M.A. Wagner, C. Besler, G. Gerstenecker, R. Zhang, X.M. Li, A.J. DiDonato, V. Gogonea, W.H. Tang, J.D. Smith, E.F. Plow, P.L. Fox, D.M. Shih, A.J. Lusis, E.A. Fisher, J.A. DiDonato, U. Landmesser, S.L. Hazen, Myeloperoxidase, paraoxonase-1, and HDL form a functional ternary complex, J. Clin. Investig. 123 (2013) 3815–3828.
[29] S.J. Nicholls, S.L. Hazen, The role of myeloperoxidase in the pathogenesis of coronary artery disease, Jpn. J. Infect. Dis. 57 (2004) S21–S22.
[30] J. Wu, Z. He, X. Gao, F. Wu, R. Ding, Y. Ren, Q. Jiang, M. Fan, C. Liang, Z. Wu, Oxidized high-density lipoprotein impairs endothelial progenitor cells' function by activation of CD36-MAPK-TSP-1 pathways, Antioxid. Redox Signal. 22 (2015) 308–324.
[31] S.A. Sorrentino, C. Besler, L. Rohrer, M. Meyer, K. Heinrich, F.H. Bahlmann, M. Mueller, T. Horvath, C. Doerries, M. Heinemann, S. Flemmer, A. Markowski, C. Manes, M.J. Bahr, H. Haller, A. von Eckardstein, H. Drexler, U. Landmesser, Endothelial-vasoprotective effects of high-density lipoprotein are impaired in patients with type 2 diabetes mellitus but are improved after extended-release niacin therapy, Circulation 121 (2010) 110–122.
[32] G.M. Anantharamaiah, Synthetic peptide analogs of apolipoproteins, Methods Enzymol. 128 (1986) 627–647.
[33] S.T. Reddy, M. Navab, G.M. Anantharamaiah, A.M. Fogelman, Apolipoprotein A-I mimetics, Curr. Opin. Lipidol. 25 (2014) 304–308.
[34] M. Navab, S.T. Reddy, G.M. Anantharamaiah, S. Imaizumi, G. Hough, S. Hama, A.M. Fogelman, Intestine may be a major site of action for the apoA-I mimetic peptide 4F whether administered subcutaneously or orally, J. Lipid Res. 52 (2011) 1200–1210.
[35] M. Navab, G.M. Anantharamaiah, S. Hama, D.W. Garber, M. Chaddha, G. Hough, R. Lallone, A.M. Fogelman, Oral administration of an Apo A-I mimetic Peptide synthesized from D-amino acids dramatically reduces atherosclerosis in mice independent of plasma cholesterol, Circulation 105 (2002) 290–292.
[36] G.S. Getz, C.A. Reardon, Apolipoprotein A-I and A-I mimetic peptides: a role in atherosclerosis, J. Inflamm. Res. 4 (2011) 83–92.
[37] G. Datta, M. Chaddha, S. Hama, M. Navab, A.M. Fogelman, D.W. Garber, V.K. Mishra, R.M. Epand, R.F. Epand, S. Lund-Katz, M.C. Phillips, J.P. Segrest, G.M. Anantharamaiah, Effects of increasing hydrophobicity on the physical-chemical and biological properties of a class A amphipathic helical peptide, J. Lipid Res. 42 (2001) 1096–1104.
[38] M. Navab, G.M. Anantharamaiah, S.T. Reddy, S. Hama, G. Hough, V.R. Grijalva, N. Yu, B.J. Ansell, G. Datta, D.W. Garber, A.M. Fogelman, Apolipoprotein A-I mimetic peptides, Arterioscler. Thromb. Vasc. Biol. 25 (2005) 1325–1331.
[39] C.R. White, D.W. Garber, G.M. Anantharamaiah, Anti-inflammatory and cholesterol-reducing properties of apolipoprotein mimetics: a review, J. Lipid Res. 55 (2014) 2007–2021.
[40] S. Sharma, S. Umar, F. Potus, A. Iorga, G. Wong, D. Meriwether, S. Breuils-Bonnet, D. Mai, K. Navab, D. Ross, M. Navab, S. Provencher, A.M. Fogelman, S. Bonnet, S.T. Reddy, M. Eghbali, Apolipoprotein A-I mimetic peptide 4F rescues pulmonary hypertension by inducing microRNA-193-3p, Circulation 130 (2014) 776–785.
[41] D. Meriwether, D. Sulaiman, A. Wagner, V. Grijalva, I. Kaji, K.J. Williams, L. Yu, S. Fogelman, C. Volpe, S.J. Bensinger, G.M. Anantharamaiah, I. Shechter, A.M. Fogelman, S.T. Reddy, Transintestinal transport of the anti-inflammatory drug 4F and the modulation of transintestinal cholesterol efflux, J. Lipid Res. 57 (2016) 1175–1193.
[42] S.T. Reddy, M. Navab, G.M. Anantharamaiah, A.M. Fogelman, Searching for a successful HDL-based treatment strategy, Biochim. Biophys. Acta 1841 (2014) 162–167.
[43] A. Chattopadhyay, M. Navab, G. Hough, F. Gao, D. Meriwether, V. Grijalva, J.R. Springstead, M.N. Palgnachari, R. Namiri-Kalantari, F. Su, B.J. Van Lenten, A.C. Wagner, G.M. Anantharamaiah, R. Farias-Eisner, S.T. Reddy, A.M. Fogelman, A novel approach to oral apoA-I mimetic therapy, J. Lipid Res. 54 (2013) 995–1010.
[44] L.T. Bloedon, R. Dunbar, D. Duffy, P. Pinell-Salles, R. Norris, B.J. DeGroot, R. Movva, M. Navab, A.M. Fogelman, D.J. Rader, Safety, pharmacokinetics, and pharmacodynamics of oral apoA-I mimetic peptide D-4F in high-risk cardiovascular patients, J. Lipid Res. 49 (2008) 1344–1352.
[45] S. Imaizumi, M. Navab, C. Morgantini, C. Charles-Schoeman, F. Su, F. Gao, M. Kwon, E. Ganapathy, D. Meriwether, R. Farias-Eisner, A.M. Fogelman, S.T. Reddy, Dysfunctional high-density lipoprotein and the potential of apolipoprotein A-1 mimetic peptides to normalize the composition and function of lipoproteins, Circ. J. 75 (2011) 1533–1538.
[46] B.J. Van Lenten, A.C. Wagner, C.L. Jung, P. Ruchala, A.J. Waring, R.I. Lehrer, A.D. Watson, S. Hama, M. Navab, G.M. Anantharamaiah, A.M. Fogelman, Anti-inflammatory apoA-I-mimetic peptides bind oxidized lipids with much higher affinity than human apoA-I, J. Lipid Res. 49 (2008) 2302–2311.
[47] M. Navab, S.T. Reddy, G.M. Anantharamaiah, G. Hough, G.M. Buga, J. Danciger, A.M. Fogelman, D-4F-mediated reduction in metabolites of arachidonic and linoleic acids in the small intestine is associated with decreased inflammation in low-density lipoprotein receptor-null mice, J. Lipid Res. 53 (2012) 437–445.
[48] L. Zheng, M. Settle, G. Brubaker, D. Schmitt, S.L. Hazen, J.D. Smith, M. Kinter, Localization of nitration and chlorination sites on apolipoprotein A-I catalyzed by myeloperoxidase in human atheroma and associated oxidative impairment in ABCA1-dependent cholesterol efflux from macrophages, J. Biol. Chem. 280 (2005) 38–47.
[49] E.A. Jaffe, R.L. Nachman, C.G. Becker, C.R. Minick, Culture of human endothelial cells derived from umbilical veins. Identification by morphologic and immunologic criteria, J. Clin. Investig. 52 (1973) 2745–2756.
[50] C. Wu, S.B. Asokan, M.E. Berginski, E.M. Haynes, N.E. Sharpless, J.D. Griffith, S.M. Gomez, J.E. Bear, Arp2/3 is critical for lamellipodia and response to extracellular matrix cues but is dispensable for chemotaxis, Cell 148 (2012) 973–987.
[51] C. Chen, J.T. Hu, Y.J. Tu, J.C. Wu, J. Liang, L.L. Gao, Z.G. Wang, B.F. Yang, D.L. Dong, Effects of isosorbide mononitrate on the restoration of injured artery in mice in vivo, Eur. J. Pharmacol. 640 (2010) 150–156.
[52] S. Miura, M. Fujino, Y. Matsuo, A. Kawamura, H. Tanigawa, H. Nishikawa, K. Saku, High density lipoprotein-induced angiogenesis requires the activation of Ras/MAP kinase in human coronary artery endothelial cells, Arterioscler. Thromb. Vasc. Biol. 23 (2003) 802–808.
[53] W. Zhu, S. Saddar, D. Seetharam, K.L. Chambliss, C. Longoria, D.L. Silver, I.S. Yuhanna, P.W. Shaul, C. Mineo, The scavenger receptor class B type I adaptor protein PDZK1 maintains endothelial monolayer integrity, Circ. Res. 102 (2008) 480–487.
[54] B. Shao, C. Bergt, X. Fu, P. Green, J.C. Voss, M.N. Oda, J.F. Oram, J.W. Heinecke, Tyrosine 192 in apolipoprotein A-I is the major site of nitration and chlorination by myeloperoxidase, but only chlorination markedly impairs ABCA1-dependent cholesterol transport, J. Biol. Chem. 280 (2005) 5983–5993.
[55] D.Q. Peng, G. Brubaker, Z. Wu, L. Zheng, B. Willard, M. Kinter, S.L. Hazen, J.D. Smith, Apolipoprotein A-I tryptophan substitution leads to resistance to myeloperoxidase-mediated loss of function, Arterioscler. Thromb. Vasc. Biol. 28 (2008) 2063–2070.
[56] J. Ou, J. Wang, H. Xu, Z. Ou, M.G. Sorci-Thomas, D.W. Jones, P. Signorino, J.C. Densmore, S. Kaul, K.T. Oldham, K.A. Pritchard Jr., Effects of D-4F on vasodilation and vessel wall thickness in hypercholesterolemic LDL receptor-null and LDL receptor/apolipoprotein A-I double-knockout mice on Western diet, Circ. Res. 97 (2005) 1190–1197.
[57] C.R. White, G. Datta, A.K. Buck, M. Chaddha, G. Reddy, L. Wilson, M.N. Palgunachari, M. Abbasi, G.M. Anantharamaiah, Preservation of biological function despite oxidative modification of the apolipoprotein A-I mimetic peptide 4F, J. Lipid Res. 53 (2012) 1576–1587.
[58] B.A. Hall, J.P. Armitage, M.S. Sansom, Transmembrane helix dynamics of bacterial chemoreceptors supports a piston model of signalling, PLoS Comput. Biol. 7 (2011) e1002204.
[59] D.R. Janero, Malondialdehyde and thiobarbituric acid-reactivity as diagnostic indices of lipid peroxidation and peroxidative tissue injury, Free Radic. Biol. Med. 9 (1990) 515–540.
[60] M.A. Rosenbaum, P. Chaudhuri, B. Abelson, B.N. Cross, L.M. Graham, Apolipoprotein A-I mimetic peptide reverses impaired arterial healing after injury by reducing oxidative stress, Atherosclerosis 241 (2015) 709–715.
[61] I. Gonçalves, A. Edsfeldt, N.Y. Ko, H. Grufman, K. Berg, H. Björkbacka, M. Nitulescu, A. Persson, M. Nilsson, C. Prehn, J. Adamski, J. Nilsson, Evidence Supporting a Key Role of Lp-PLA2-Generated Lysophosphatidylcholine in Human Atherosclerotic PlaqueInflammation, . Atertio Thromb. Vasc. Biol. 32 (2012) 1505–1512.
[62] M.A. Rosenbaum, P. Chaudhuri, B. Abelson, B.N. Cross, L.M. Graham, Apolipoprotein A-I mimetic peptide reverses impaired arterial healing after injury by reducing oxidative stress, Atherosclerosis 241 (2015) 709–715.
[63] G.M. Anantharamaiah, V.K. Mishra, D.W. Garber, G. Datta, S.P. Handattu, M.N. Palgunachari, M. Chaddha, M. Navab, S.T. Reddy, J.P. Segrest, A.M. Fogelman, Structural requirements for antioxidative and anti-inflammatory properties of apolipoprotein A-I mimetic peptides, J. Lipid Res. 48 (2007) 1915–1923.
[64] J. Liu, S. Yao, S. Wang, P. Jiao, G. Song, Y. Yu, P. Zhu, S. Qin, D-4F, an apolipoprotein A-I mimetic peptide, protects human umbilical vein endothelial cells from oxidized low-density lipoprotein-induced injury by preventing the downregulation of pigment epithelium-derived factor expression, J. Cardiovasc. Pharmacol. 63 (2014) 553–561.
[65] J.A. van Aalst, D.M. Zhang, K. Miyazaki, S.M. Colles, P.L. Fox, L.M. Graham, Role of reactive oxygen species in inhibition of endothelial cell migration by oxidized low-density lipoprotein, J. Vasc. Surg. 40 (2004) 1208–1215.
[66] N. Yang, S. Yao, M. Wang, P. Jiao, Y. Zhang, S. Qin, Apolipoprotein A-I mimetic peptide reverse D-4F improves the biological functions of mouse bone marrow-derived late EPCs via PI3K/AKT/eNOS pathway, Mol. Cell Biochem. 377 (2013) 229–236.
[67] S.J. Peterson, D. Husney, A.L. Kruger, R. Olszanecki, F. Ricci, L.F. Rodella, A. Stacchiotti, R. Rezzani, J.A. McClung, W.S. Aronow, S. Ikehara, N.G. Abraham, Long-term treatment with the apolipoprotein A1 mimetic peptide increases

antioxidants and vascular repair in type I diabetic rats, J. Pharmacol. Exp. Ther. 322 (2007) 514–520.
[68] M. Navab, G.M. Anantharamaiah, S.T. Reddy, B.J. Van Lenten, A.C. Wagner, S. Hama, G. Hough, E. Bachini, D.W. Garber, V.K. Mishra, M.N. Palgunachari, A.M. Fogelman, An oral apoJ peptide renders HDL antiinflammatory in mice and monkeys and dramatically reduces atherosclerosis in apolipoprotein E-null mice, Arterioscler. Thromb. Vasc. Biol. 25 (2005) 1932–1937.
[69] X. Song, P. Fischer, X. Chen, C. Burton, J. Wang, An apoA-I mimetic peptide facilitates off-loading cholesterol from HDL to liver cells through scavenger receptor BI, Int. J. Biol. Sci. 5 (2009) 637–646.
[70] M. Navab, G.M. Anantharamaiah, S.T. Reddy, S. Hama, G. Hough, V.R. Grijalva, A.C. Wagner, J.S. Frank, G. Datta, D. Garber, A.M. Fogelman, Oral D-4F causes formation of pre-beta high-density lipoprotein and improves high-density lipoprotein-mediated cholesterol efflux and reverse cholesterol transport from macrophages in apolipoprotein E-null mice, Circulation 109 (2004) 3215–3220.
[71] L.E. Smythies, C.R. White, A. Maheshwari, M.N. Palgunachari, G.M. Anantharamaiah, M. Chaddha, A.R. Kurundkar, G. Datta, Apolipoprotein A-I mimetic 4F alters the function of human monocyte-derived macrophages, Am. J. Physiol. Cell Physiol. 298 (2010) C1538–C1548.
[72] V.K. Mishra, M.N. Palgunachari, D.T. McPherson, G.M. Anantharamaiah, Lipid complex of apolipoprotein A-I mimetic peptide 4F is a novel platform for paraoxonase-1 binding and enhancing its activity and stability, Biochem. Biophys. Res. Commun. 430 (2013) 975–980.
[73] C. Besler, K. Heinrich, L. Rohrer, C. Doerries, M. Riwanto, D.M. Shih, A. Chroni, K. Yonekawa, S. Stein, N. Schaefer, M. Mueller, A. Akhmedov, G. Daniil, C. Manes, C. Templin, C. Wyss, W. Maier, F.C. Tanner, C.M. Matter, R. Corti, C. Furlong, A.J. Lusis, A. von Eckardstein, A.M. Fogelman, T.F. Luscher, U. Landmesser, Mechanisms underlying adverse effects of HDL on eNOS-activating pathways in patients with coronary artery disease, J. Clin. Investig. 121 (2011) 2693–2708.
[74] B. Hewing, S. Parathath, T. Barrett, W.K. Chung, Y.M. Astudillo, T. Hamada, B. Ramkhelawon, T.C. Tallant, M.S. Yusufishaq, J.A. Didonato, Y. Huang, J. Buffa, S.Z. Berisha, J.D. Smith, S.L. Hazen, E.A. Fisher, Effects of native and myeloperoxidase-modified apolipoprotein a-I on reverse cholesterol transport and atherosclerosis in mice, Arterioscler. Thromb. Vasc. Biol. 34 (2014) 779–789.